ASTRONOMY & ASTROPHYSICS
SUPPLEMENT SERIES

Astron. Astrophys. Suppl. Ser. **78**, 249-268 (1989)

Photometric calibration of the APM Proper Motion Project

D. W. Evans

Institute of Astronomy, Madingley Road, Cambridge CB3 0HA, U.K.

Received November 24, 1988 ; accepted February 1, 1989

Summary. — Deep *BVR* photometry is presented in the magnitude range $11 < B < 21$ obtained using a CCD camera. These magnitudes are used to calibrate the photographic photometry of the APM Proper Motion Project. Useful colour-colour relationships are also presented calculated using the stellar spectra contained in Gunn and Stryker (1983).

Key words : photometry — stars.

1. Introduction.

This paper gives details of the photometric calibrations carried out for the APM Proper Motion Project. This project is a major study of Galactic structure and kinematics based on photographic astrometry and photometry. The photographic plates were taken using the UK and Palomar Schmidt telescopes and were measured using the APM (Automated Plate Measuring) facility in Cambridge. The photometry was calibrated using CCD sequences in *B, V* and *R* in the magnitude range $11 < B < 21$. These sequences are presented along with finding charts.

Work has also been carried out in deriving synthetic colour-colour relationships. Most of the photographic photometry for this project is in the form of *O* and *E* magnitudes from the Palomar Observatory Sky Survey (POSS) plates. In order to compare these magnitudes with the more commonly quoted ones, e.g. Johnson *B* and *V*, the spectra contained in Gunn and Stryker (1983) have been convolved with various passbands to produce the required relationships.

2. The choice of fields.

Four fields were used in this project covering a total sky area of approximately 90 square degrees. The positions and details of these fields are given in table I.

Photometry for a fifth field (13^h25^m, $-30°$) was also taken during the CCD observing trip and is included in this paper (Tab. VII). No photographic plates were obtained for this field and thus is not included in the rest of the project.

The following criteria were used for determining which fields to work in.

a) Both plate epochs, POSS for primary epoch and UKST (UK Schmidt telescope) secondary, should be immediately available. The plate centres from the two telescopes should be close to ensure a large overlap. Quite a few fields were rejected due to the centre of one plate being on the edge of another. Due to the way that these Schmidt surveys were undertaken this meant that large sections of sky could not be used unless plates were available with non-standard plate centres, which was not usually the case.

b) The fields should be in areas of low obscuration. This was determined from Burstein and Heiles (1982) and basically restricted us to $|b| > 30°$ (see Tab. I).

c) The declinations of the fields should be within 20° of the celestial equator. This meant that all telescopes used in the project could observe the fields without having to go more than about 50° from the zenith. Similarly a restriction existed in right ascensions due to the CCD observing trip being in March. This restricted the positions to between 8^h and 16^h.

d) Estimates of the magnitude and direction of the Solar Motion could be derived from the fields. To do this the fields must not be too close to the solar apex/antapex (where the motion is almost purely radial) and reasonably, well spread out so that the position of the apex could be obtained "by triangulation".

e) To measure Oort's constants of differential rotation the fields should have a good spread in galactic longitude and have varied values of sin 2*l* and cos 2*l*. To ensure that the Oort motion is a large as possible the galactic latitude should be as small as possible (i.e. large cos *b*) consistent with the obscuration restriction. This can be seen by inspecting the equations for the proper motion components of differential galactic rotation,

$$\mu_{l_c} = (A \cos 2l + B) \cos b, \quad (1)$$

$$\mu_b = -A \sin 2l \cos b \sin b, \quad (2)$$

where μ_{l_c} and μ_{b_c} are the proper motion components measured on great circles in the direction of increasing galactic longitude and latitude respectively, l and b the galactic coordinates, and A and B the Oort constants.

The photographic plate material used for the primary epoch (~ 1950) plates were glass copies of plates taken as part of the National Geographic Society-Palomar Sky Survey. The secondary epoch (~ 1980) plates were taken on the UK Schmidt Telescope for a variety of projects. A list of the plates used for this project is given in table II.

In each of the four fields two regions were selected by eye and had CCD frames taken of them. These regions were chosen for the large number of stars and even spread of magnitudes within them. The second point was to ensure that our technique of calibrating the long exposure CCD frame from the short and medium exposure ones would work. The two regions were chosen not to be near to each other or the edge of the plate, so as to minimize field effects in the calibration of the Schmidt plates.

3. The CCD observations.

These were taken using the 1 metre SAAO (South African Astronomical Observatory) telescope which is situated at Sutherland, South Africa (32°22′46″ S, 20°48′39″ E). For details concerning the telescope consult Glass (1982). The UCL-SAAO charge coupled device (CCD) camera system (Walker *et al.*, 1984) is situated at the Cassegrain focus with a focal ratio of $f/15.8$ and a scale of approximately 12.″8/mm. Using the RCA CCD device this gives a frame size of about 2′× 3′ and a pixel size of about 0.″4 square.

The observations were carried out during the period 19th to 23rd March 1985 and of these five nights, three where photometric. Although the other two nights were non-photometric they were not totally clouded over for the whole time, so long exposure CCD frames could be taken and calibrated from shorter exposures taken of the same region on one of the photometric nights.

On the photometric nights the calibration of the CCD frames was achieved by taking short exposure frames of E field standard stars (Menzies *et al*, 1980) as close as possible in time to the object CCD exposures. For each CCD field at least 8 exposures were taken. The filters used were B, V and R broadband filters, which correspond approximately to the Johnson B and V and Cousins R standard systems. In both B and R there were three exposures : ~ 10s, ~ 200s and ~ 2000s. While in V only two exposures were taken, ~ 10s and ~ 200s.

Since this data was intended to calibrate the O and E data from the Palomar Observatory Sky Survey (POSS) plates, the V exposures were only necessary to produce the colour corrections to transform from the natural B and R system of the CCD filters to that of the standard magnitude system. To do this only short V exposures were required and therefore not much additional telescope time and effort was needed. A transformation to go from B, V (natural) to B, V (standard) already existed. Combining this with my B, V and R data a B, R transformation was obtained for use on the B and R deep frames.

The standard transformations that are normally used (A.R. Walker, private communication) are,

$$V = V_{\rm CCD} - 0.051\,(B-V)_{\rm CCD}, \quad (3)$$

$$(B-V) = 1.112\,(B-V)_{\rm CCD}, \quad (4)$$

$$(V-R) = 0.927\,(V-R)_{\rm CCD}, \quad (5)$$

where the CCD subscript denotes the natural photometric system of the CCD filters. Rearranging these transformations the following two equations are obtained :

$$B = B_{\rm CCD} + 0.061\,(B-V)_{\rm CCD}, \quad (6)$$

$$(B-R) = 0.927\,(B-R)_{\rm CCD} + 0.185\,(B-V)_{\rm CCD}. \quad (7)$$

Using the CCD data we can deduce the relationship between $(B-V)_{\rm CCD}$ and $(B-R)_{\rm CCD}$. This is shown in figure 1. Linear regression produces the following equation,

$$(B-V)_{\rm CCD} = 0.575(\pm 0.016)(B-R)_{\rm CCD} + 0.042(\pm 0.020). \quad (8)$$

It should be noted that for stars redder than $M0$, $(B-V) = 1.45$, this relationship is unlikely to be accurate.

Using equations 6, 7 and 8 we obtain

$$B = B_{\rm CCD} + 0.035(\pm 0.001)(B-R)_{\rm CCD} + 0.003(\pm 0.001), \quad (9)$$

$$(B-R) = 1.033(\pm 0.003)(B-R)_{\rm CCD} + 0.008(\pm 0.004), \quad (10)$$

which were the transformations used for the B and R magnitudes. The errors quoted in these equations are rms errors.

The flat-fielding and the various subtractions (bias, dark current and preflash) were carried out in Cape Town, while the remainder of the reductions (calculation of total intensities and conversion to calibrated magnitudes) were carried out in Cambridge.

4. The CCD sequences.

For each field there are about 15 to 25 stars with B and R magnitudes and about 15 with V magnitudes. Tables III to VII give the sequences and figures 2 to 6 are the corresponding finding charts. These magnitudes were calculated from weighted averages of the total intensities of

1989A&AS...78..249E

the images from the different exposures. No image was used with a peak intensity of greater than 20,000 cf. saturation level of $\sim 32,000$.

Two regions have been measured twice (on different nights) so that an estimate of the sequence errors, random and systematic, can be made. In tables III to VII the average values of the magnitudes of these stars has been noted. These stars are marked as having been measured twice.

Figure 7 shows this comparison for the stars in one of these regions (the second region of the 8 Hour Field). This gave the result that the random error of the photometry (down to $20^{\rm m}$) was 0.03 magnitude for B, V and R. The accuracy of the zero point was estimated to be better than 0.03 magnitude. Therefore taken as a whole the overall accuracy of these data is estimated to be 0.05 magnitude.

5. Calibration technique.

To calibrate the APM magnitudes it is intended that only a linear transformation and a colour term, to account for differences between the standard (B, R) and photographic (O, E) wavebands, is required. This is due to a linearizing algorithm that has been applied to the APM data (Bunclark and Irwin, 1983). In practice it has been found that a small quadratic term is also needed in the transformation. This non-linearity is due to the scanner's spot halo. The effect of the scanning laser on an image is very similar to atmospheric seeing in that it smears out the image. The halo surrounding the central region of the laser spot makes this convolution more complicated and affects the photometry of many objects (Cawson *et al.,* 1987). The main way it affects the linearizing algorithm is that this convolution comes after the transformation from intensity to photographic density (i.e. the exposure) and causes the profile of a star to be slightly dependent on magnitude. This means that after "linearizing" the magnitude system there still remains a slight curvature which if not taken into account would lead to systematic errors of order 0.2 magnitude in the photometry. An unfortunate side-effect of using a quadratic terms is that extrapolation beyond the limits of the CCD sequence requires caution. Further than ~ 1 magnitude away from the CCD sequence limits the calibration will start to become unreliable. Table I gives the photometric limits for the 4 fields used in this project.

No published transformation between the standard photoelectric and the POSS photographic photometry systems exists cf. Blair and Gilmore (1982). To calculate these transformation colour terms all 4 fields were calibrated using the CCD standards but without using a colour term i.e. assuming that the two systems are the same. The residuals (CCD standard magnitudes – calibrated photographic magnitudes) were plotted against CCD colour and a linear least-squares fit was used to derive the colour term (see Fig. 8). The results from these fits are :

$$B - O = (-0.135 \pm 0.03) \times (B - R), \qquad (11)$$

$$R - E = (0.00 \pm 0.02) \times (B - R). \qquad (12)$$

These equations yield a colour-colour transformation of,

$$(O - E)_{\rm POSS} = (1.135 \pm 0.035) \times (B - R). \qquad (13)$$

Equations 11 and 12 were used to convert the (B, R) CCD standards to the (O, E) system, which were then used to calibrate the APM magnitudes onto the same system. It should be noted that, similar to equation 8, these relationships might not be correct for stars redder than M0.

Figure 9 shows a typical comparison between CCD magnitudes and magnitudes calibrated from the APM data for the standards in one of the fields. The only deviation from the 45° line drawn in this diagram will be due to random scatter and the presence of terms higher than quadratic in the true (but unknown) transformation. The average errors are 0.09 magnitude for both O and E photographic photometry and were estimated from the scatter of the data points about the 45° lines (similar to that drawn in Fig. 9). This estimate assumes that all of the scatter is due to error in the photographic photometry and will tend to overestimate the errors.

The error in photographic colour $(O - E)$ is 0.12 magnitude and is shown in a histogram (Fig. 10) of the colour errors for the CCD standards.

It should be noted that only images classified as stars were used in these calibrations.

6. Synthetic colours.

To confirm some of the relationships derived earlier on in this paper and to provide further useful colour-colour transformations, work has been carried out on synthetic colours. Using the spectra of different types of star and convolving them with the emulsion response and the effects of atmospheric absorption, theoretical colours can be obtained. The equation used was

$$C_{(1-2)} = -2.5 \log_{10} \left(\frac{\int_0^\infty J D_1 \exp(-\kappa \sec \zeta_1) {\rm d}\lambda}{\int_0^\infty J D_2 \exp(-\kappa \sec \zeta_2) {\rm d}\lambda} \right) + {\rm constant}, \qquad (14)$$

where J is the intensity of the source, D the response of the detector, κ the exponential atmospheric absorption coefficient (all of which are functions of λ) and ζ the zenith angle (possibly different for the two responses). J is calculated from the spectral atlas of Gunn and Stryker (1983) and the values for κ comes from Allen (1973, p126). The constant is defined such that the average colour index, $C_{(1-2)}$, for the B9V, A0V and A1V stars in the spectral atlas is zero. These three spectral types are used to define the zero instead of the usual one (A0V) in order to minimize the risk of systematic error due to irregularities in the spectra and inaccuracies in the spectral classifications.

It should be noted that some of these relationships (those involving a blue passband i.e. O, B, J) can be in error by $\sim$ 0.1 for stars redder than $(O - E) \sim 2.5$ $((B{-}V) \sim 1.4)$. The reason for this, as pointed out in Gunn and Stryker (1983), is probably due to the blue region of the spectra of the reddest stars being systematically in error.

The sources for the detector responses considered in this work are Minkowski and Abell (1963) for O and E, Ažusienis and Straižys (1969) for B and V, and Bessell (1986) for R and I. For the J response there is no suitable published data. In Kron (1980) a J response is given, but has been calculated using the GG385 filter whereas the UK Schmidt uses GG395. Table VIII gives the response used in this work and has been calculated using (i) the IIIa-J emulsion response (from Kodak pamphlet No.P-14), (ii) the transmittance of GG395 (2mm) and (iii) the transmission of the UK Schmidt telescope corrector plate, which is made from Schott UBK7 and LLF6 glass. Figure 11 shows the passbands used superimposed on the spectrum of a G0V star.

For all the following calculations the airmass, $\eta = \sec\zeta$, has been taken as zero. When standard systems are set up they are all reduced to zero atmosphere. For the blue magnitudes the atmospheric extinction correction used is a function of colour (this is to take into account the variation of a star's effective wavelength as a function of colour), but for V and redder passbands a mean atmospheric extinction is used since the colour dependence of the extinction for these passbands amounts to a correction of less than 0.01^{m} (Eggen, 1950 ; Kron and Smith 1951). For the CCD standards presented in tables III to VII a mean atmospheric extinction has been used for all magnitudes, but most of the colour dependence of the atmospheric extinction has been absorbed by Equations 3 to 5 i.e. the CCD passbands include about one airmass of extinction. Similarly, when the photographic photometry is calibrated, it is effectively a mean atmospheric extinction that is used, with most of the colour dependence again being absorbed by the colour terms (Eqs. 11, 12).

When calculating synthetic colours the first order effect of atmospheric extinction (that which is corrected by the mean atmospheric extinction) is allowed for by the setting of the zero point of the colour system using A0V stars. It is the $\exp(-\kappa \sec\zeta)$ terms in equation 14 that account for the colour dependence of atmospheric extinction. In order to simplify matters, $\eta = 0$ has been used for all calculations. This will only noticeably affect a colour index which involves a blue response function (O, B and J). The effect of this simplification will be at most a shift of a few hundredths in colour for the reddest stars.

In order to test the relationships derived a comparison was carried out using the E-region standards contained in Menzies *et al.* (1980). Best fit polynomials were calculated for dwarfs and giants for the relationships $(B - R)$ *vs.* $(B - V)$ and $(R - I)$ *vs.* $(B - R)$. These relationships are given in table IX. These lines were then plotted on the same diagrams as the corresponding observed relationships from the E-region standards (see Fig. 12). The synthetic colour-colour relationships are in good agreement with the observed ones.

To confirm the relationships given in equations (11) and (12) synthetic relationships for $(B - O)$ and $(R - E)$ *vs.* $(B - R)$ were calculated. These are displayed in figure 13 along with the relation used to convert the CCD standards onto the photographic (O, E) system. The colour range of the CCD standards is $0.5 < (B - R) < 2.5$, and it is over this range which it is important for the relationships calculated from the photometry to agree with those derived from synthetic colours.

Due to the extended ultraviolet response of the O passband as compared to B (see Fig. 11) there is a substantial gradient (and kink) in the relationship between $(B - O)$ and $(B - R)$. In the range specified, the gradient agrees with that calculated from the photometry (-0.135). However, due to the kink in the relationship, there is an offset of $\sim 0.05^{\mathrm{m}}$ for the average star colour. In converting the CCD standards from B to O, this offset will mean that they will, in general, be 0.05^{m} too faint in O. Since this difference is small and the O response is uncertain to some extent no additional correction is made to the standards other than the relationship in equation (11).

Although the shapes of the E and R passbands are quite different, they have similar effective wavelengths, hence the zero gradient relationship seen in figure 13. It is only for the very red objects that there is any departure from this linear relationship. This agrees very well with the measurements made using the CCD standards.

Due to the widespread use of IIIa-J, in combination with the GG395 filter, as a recording medium in astronomy, the transformation between B and J is of interest. This transformation has been calculated using observational data in Blair and Gilmore (1982) where they find $(B - J) = (0.28 \pm 0.04) \times (B - V)$. Using the CCD standards and J plates from this project, and using the same methods used to obtain equations (11) and (12), the colour term has been derived to be $(B - J) = (0.24 \pm 0.04) \times (B - V)$. The computed relationship using stellar spectra is shown in figure 14. If a linear fit is carried out to the data points between the colour limits covered by the standards used in Blair and Gilmore (1982) a gradient of 0.23 is obtained and is in good agreement with the observations. A more accurate calculation can be done with the airmass set to zero for the B and V passbands, but set to one for J. This is more representative of the conditions under which these colour terms have been measured. When this is carried out, the gradient of the synthetic relationship increases by a few hundredths. Best fit polynomials have also been calculated (see Fig. 14) and their coefficients are given in table IX.

One of the most important relationships needed for this project is the conversion from $(O - E)$ to $(B - V)$. This is because $(B - V)$ is one of the most widely used colours in astronomy. Figure 15 shows the synthetic colour-colour diagram along with the dwarf and giant relationships (coefficients given in Tab. IX).

For three of the fields in this project there exist infrared (I) plates. In order to calibrate these, from the CCD standards, a transformation between $(B-R)$ and $(R-I)$ is required. Figure 12 (c) shows this relationship. The slight upturn at the red end of the curve is unimportant since none of the standards lie on this part of the curve. The coefficients for this polynomial and that for the $(E-I)$ to $(R-I)$ relationship are given in table IX. It should be noted that the I passband used in this work has been the I_C passband in Bessell (1986). In this paper he suggests an alternative passband (I_Z) which is claimed to be a better representation of the Cousins I passband. Since the difference between these passbands (and the I_N photographic passband) is small no correction is made. Even for the reddest stars this simplification will cause systematic errors in colour of less than 0.1^m.

A comparison was also carried out between this work and that of Bessell (1986) where the Vilnius stellar spectra (Straižys and Sviderskienė, 1972) were used. Figure 16 shows an example. In all cases the agreement was good, with the difference for the reddest stars no more than $\sim 0.1^m$. This small difference can probably be accounted for by biases in the spectra for the reddest stars.

Acknowledgements.

I thank Mike Irwin,Gerry Gilmore and Richard McMahon for useful discussions. Thanks are also due to the staff at the SAAO for providing assistance during the CCD observations. Financial support for this work was provided by the Science and Engineering Research Council.

References

ALLEN C. W. : 1973, Astrophysical Quantities, 3rd ed. (Athlone Press, London).
AŽUSIENIS A. and STRAIŽYS V. : 1969, *Soviet Astron.* **13**, 316.
BESSELL M. S. : 1986, *Publ. Astron. Soc. Pac.* **98**, 1303.
BLAIR M. and GILMORE G. : 1982, *Publ. Astron. Soc. Pac.* **94**, 742.
BUNCLARK P. S. and IRWIN M. J. : 1983, Proc. Statistical Methods in Astronomy, Ed. Rolfe, p. 195, ESA SP-201.
BURSTEIN D. and HEILES C. : 1982, *Astron. J.* **87**, 1165.
CAWSON M. G. M., KIBBLEWHITE E. J., DISNEY M. J. and PHILLIPPS S. : 1987, *Mon. No. R. Astron. Soc.* **224**, 557.
EGGEN O. J. : 1950, *Astrophys. J.* **111**, 68.
GLASS I. S. : 1982. South African Astronomical Observatory Facilities Manual, 3rd ed.
GUNN J. E. and STRYKER L. L. : 1983, *Astrophys. J. Suppl. Ser.* **52**, 121.
KRON G. E.and SMITH J.L. : 1951, *Astrophys. J.* **113**, 324.
KRON R. G. : 1980, *Astrophys. J. Suppl. Ser.* **43**, 305.
MENZIES J. W., BANFIELD R. M. and LAING J. D. : 1980, SAAO Circulars **1**, 49.
MINKOWSKI R. L. and ABELL G. O. : 1963, Basic Astronomical Data (Stars and Stellar System, Vol. 3) Ed. K. Aa.Strand, p. 481 (Univ. of Chicago Press, Chicago).
STRAIŽYS V. and SVIDERSKIENĖ Z. : 1972, Bull. Vilnius. Astron. Obs. No. 35.
WALKER D. D., WALKER A. R., SANFORD P. E., MACK P., LYONS A., FORDHAM J., BONE D. and BOKSENBERG A. : 1984. Proc. of the Eighth Symposium on Photoelectronic Image Devices, Ed. B. L. Morgan (Academic Press, London).

TABLE I. — *This shows the four fields used in the project. A_v is the total absorption in V for each field. These values are taken from Burstein and Heiles* (1982). *O_{lim} and E_{lim} refer to the limits in the O and E photometry beyond which no CCD standards were available. POSS refers to the Palomar Observatory Sky Survey field number. Similarly UKS is the UK Schmidt telescope field number. The trigonometric values in the last three columns show the suitability of these fields for measuring Oort's constants (see text).*

Name	RA		dec		l	b	A_v	O_{lim}	E_{lim}	POSS	UKS	$\sin 2l$	$\cos 2l$	$\cos b$
	h	m	°	′	°	°								
8 Hour Field	8	53	17	30	210	35	0.05	11.6-21.1	9.6-19.8	62	—	0.87	0.50	0.82
11 Hour Field	11	12	-20	00	274	37	0.10	12.9-20.2	12.1-18.8	1558	570	-0.14	-0.99	0.80
12 Hour Field	12	05	11	30	268	71	0.00	12.7-19.9	11.5-18.5	1385	—	0.07	-1.00	0.33
15 Hour Field	15	00	0	00	357	48	0.15	12.8-20.7	11.1-19.4	1613	868	-0.10	0.99	0.67

TABLE II. — *A list of plates used for this project.*

Plate Name	Plate Centre h m ° ′	Date	Emulsion	Filter	Plate Type	Telescope	Exposure minutes	Seeing ″
8 Hour Field (Total overlap 29 square degrees)								
J6814	8 53 17 38	8-3-1981	IIIaJ	GG395	Original	UK Schmidt	62.5	2.6
J6644	8 53 17 38	14-12-1980	IIIaJ	GG395	Original	UK Schmidt	65	3.0
O62	8 53 17 38	21-3-1950	103aO	–	Copy	Palomar Schmidt	12	3.4
E62	8 53 17 38	21-3-1950	103aE	2444	Copy	Palomar Schmidt	45	3.4
I8343	8 53 17 38	5-1-1983	IV N	RG715	Original	UK Schmidt	90	3.9
11 Hour Field (Total overlap 16 square degrees)								
J4205	11 12 -20 00	29-4-1978	IIIaJ	GG395	Copy	UK Schmidt	70	2.4
O1558	11 17 -18 31	9-3-1956	103aO	–	Copy	Palomar Schmidt	8	3.9
E1558	11 17 -18 31	9-3-1956	103aE	2444	Copy	Palomar Schmidt	45	3.1
12 Hour Field (Total overlap 32 square degrees)								
J7781	12 05 11 29	24-5-1982	IIIaJ	GG395	Original	UK Schmidt	55	2.7
O1385	12 05 11 27	13-4-1955	103aO	–	Copy	Palomar Schmidt	12	3.4
E1385	12 05 11 27	13-4-1955	103aE	2444	Copy	Palomar Schmidt	50	3.0
I8383	12 05 11 29	6-2-1983	IV N	RG715	Original	UK Schmidt	90	3.3
15 Hour Field (Total overlap 16 square degrees)								
J5779	15 00 0 00	20-3-1980	IIIaJ	GG395	Copy	UK Schmidt	70	2.6
V8570	15 00 0 00	11-5-1983	IIaD	GG495	Original	UK Schmidt	15	2.7
B8571	15 00 0 00	11-5-1983	IIaO	GG385	Original	UK Schmidt	15	2.9
O1613	14 53 -0 23	28-4-1957	103aO	–	Copy	Palomar Schmidt	8	4.0
E1613	14 53 -0 23	28-4-1957	103aE	2444	Copy	Palomar Schmidt	50	3.3
I9396	15 00 0 00	7-6-1984	IV N	RG715	Original	UK Schmidt	90	2.9

TABLE III. — *The CCD photometry for the* 8 *Hour Field. The positions are equinox* 1950. *The B and V magnitudes are in the Johnson system while the R magnitudes are in the Cousins system. The finding charts for this field are in figure* 2.

	R.A.	dec.	B	V	R	Notes
1	8 54 12.1	16 25 21	19.11		17.90	NS
2	8 54 11.2	16 25 58	15.44	14.51	14.05	
3	8 54 10.9	16 25 29	20.87		18.40	NS
4	8 54 8.3	16 26 50	19.62	18.54	17.88	
5	8 54 7.6	16 25 51	16.32	15.58	15.17	
6	8 54 7.4	16 26 40	20.92		18.50	
7	8 54 6.9	16 25 15	13.35	12.36	11.89	
8	8 54 5.2	16 26 33	12.02	11.43	11.12	
9	8 54 5.4	16 25 31	16.22	15.51	15.14	
10	8 53 30.3	18 19 53	18.22	17.28	16.82	
11	8 53 29.3	18 19 32	11.37	10.18	9.61	*
12	8 53 27.7	18 18 50	20.34		19.84	*
13	8 53 27.5	18 19 34	16.80	16.17	15.81	
14	8 53 26.1	18 18 40	16.57	16.02	15.76	*
15	8 53 26.0	18 19 7	20.75		18.48	*
16	8 53 24.5	18 19 21	12.19	11.60	11.30	*
17	8 53 23.2	18 18 10	19.39		17.90	* NS
18	8 53 20.6	18 18 5	18.45	17.70	17.23	*
19	8 53 19.6	18 19 24	17.92	17.02	16.49	*
20	8 53 19.3	18 18 52	19.86	18.36	17.63	*
21	8 53 19.0	18 19 4	21.67		18.74	
22	8 53 17.8	18 18 55	14.92	14.32	14.00	*
23	8 53 16.6	18 18 58	20.10		17.99	

Notes
* Image was measured twice.
NS Image classified as non-stellar from APM scans of UK Schmidt plates.

TABLE IV. — *The CCD photometry for the* 11 *Hour Field. The positions are equinox* 1950. *The B and V magnitudes are in the Johnson system while the R magnitudes are in the Cousins system. The finding charts for this field are in figure* 3.

	R.A.	dec.	B	V	R	Notes
1	11 14 5.7	-20 10 52	13.40	12.78	12.47	
2	11 14 5.0	-20 11 51	17.52	16.80	16.49	NS
3	11 14 3.2	-20 11 54	15.15	14.53	14.22	
4	11 14 2.2	-20 10 55	17.57	16.88	16.51	
5	11 14 1.9	-20 10 27	19.99		18.65	
6	11 14 1.4	-20 11 10	11.40	9.79		
7	11 13 59.2	-20 10 37	14.24	13.56	13.27	*
8	11 13 57.3	-20 10 40	18.24	17.54	17.08	NS
9	11 13 57.3	-20 10 49	14.33	13.63	13.31	NS
10	11 9 12.9	-19 25 52	20.75		19.65	
11	11 9 11.8	-19 25 14	20.87		19.47	NS
12	11 9 11.3	-19 24 55	21.26		18.58	
13	11 9 10.4	-19 24 45	13.62	13.00	12.71	
14	11 9 10.0	-19 24 24	19.10	18.09	17.55	
15	11 9 9.3	-19 25 1	17.25	16.42	16.03	
16	11 9 9.3	-19 25 33	18.07	17.42	17.11	
17	11 9 8.6	-19 24 16	21.42		18.80	
18	11 9 7.1	-19 25 9	18.38	17.57	17.16	
19	11 9 4.4	-19 25 47	16.69	16.11	15.78	
20	11 9 3.5	-19 25 36	15.31	14.32	13.83	
21	11 9 3.2	-19 24 20	16.86	16.02	15.61	
22	11 9 2.5	-19 25 10	17.43	16.37	15.81	
23	11 9 2.1	-19 25 13	12.76	12.30	12.09	
24	11 9 1.4	-19 24 40	18.59	17.27	16.58	

Notes
* Double star, separation 3.″5
NS Image classified as non-stellar from APM scans of UK Schmidt plates.

TABLE V. — *The CCD photometry for the 12 Hour Field. The positions are equinox 1950. The B and V magnitudes are in the Johnson system while the R magnitudes are in the Cousins system. The finding charts for this field are in figure 4.*

	R.A.	dec.	B	V	R	Notes
1	12 10 42.2	12 12 9	21.33		20.47	
2	12 10 41.8	12 11 59	20.37		19.25	NS
3	12 10 41.2	12 13 29	19.27	18.62	18.41	
4	12 10 40.6	12 13 50	17.16	15.91	15.26	
5	12 10 40.1	12 13 22	21.06		20.49	
6	12 10 38.3	12 13 16	14.47	13.74	13.41	NS
7	12 10 38.3	12 12 15	12.52	11.86	11.53	
8	12 10 37.5	12 13 10	17.09	16.09	15.57	NS
9	12 10 33.2	12 13 2	10.58	9.76		* NS
10	12 10 32.6	12 13 38	18.72	17.74	17.03	NS
11	12 10 32.5	12 12 22	15.04	14.37	14.08	
12	12 9 53.1	12 28 16	14.30	12.84	11.85	
13	12 9 52.7	12 29 32	16.27	15.43	14.93	
14	12 9 51.9	12 29 20	17.86	17.35	16.99	
15	12 9 51.1	12 28 1	18.67	17.68	16.96	
16	12 9 50.7	12 28 9	19.09	18.44	17.75	
17	12 9 49.3	12 28 6	14.95	14.29	13.91	
18	12 9 47.9	12 27 57	19.72		18.45	
19	12 9 43.2	12 29 17	13.47	12.90	12.57	

Notes

* Double star, separation 7″

NS Image classified as non-stellar from APM scans of UK Schmidt plates.

TABLE VI. — *The CCD photometry for the 15 Hour Field. The positions are equinox 1950. The B and V magnitudes are in the Johnson system while the R magnitudes are in the Cousins system. The finding charts for this field are in figure 5.*

	R.A.	dec.	B	V	R	Notes
1	14 56 15.3	-0 20 50	21.55	20.31	19.94	
2	14 56 14.2	-0 20 48	21.42		21.08	
3	14 56 14.2	-0 22 9	15.91	15.09	14.72	*
4	14 56 14.0	-0 21 48	19.19	17.74	17.20	
5	14 56 11.3	-0 21 46	12.99	12.48	12.21	
6	14 56 10.4	-0 21 58	21.33	20.73	20.52	
7	14 56 9.8	-0 21 44	15.63	14.84	14.49	
8	14 56 9.1	-0 22 11	20.56	19.70	19.38	
9	14 56 8.5	-0 21 18	11.33	9.75		
10	14 56 7.8	-0 22 35	17.25	16.52	16.19	
11	14 56 6.9	-0 21 22	19.91	18.90	18.37	
12	14 56 6.8	-0 21 41	15.61	15.14	14.92	
13	14 56 5.2	-0 22 20	18.45	17.15	16.35	
14	14 53 12.8	-1 28 12	16.13	15.29	14.90	
15	14 53 12.4	-1 28 28	18.13	17.54	17.21	
16	14 53 11.4	-1 29 10	17.32	16.38	15.90	
17	14 53 10.6	-1 28 15	20.89		19.22	NS
18	14 53 10.5	-1 28 25	15.61	14.84	14.51	
19	14 53 9.7	-1 27 45	17.94	17.15	16.66	
20	14 53 8.6	-1 28 0	16.42	15.29	14.72	
21	14 53 7.3	-1 28 1	20.18		19.02	
22	14 53 6.2	-1 27 51	21.40		20.48	
23	14 53 5.7	-1 28 41	14.20	13.63	13.36	
24	14 53 5.3	-1 29 11	12.63		11.08	

Notes

* Double star, separation 4″.5

NS Image classified as non-stellar from APM scans of UK Schmidt plates.

TABLE VII. — *The CCD photometry for the Additional Field* (13^h25^m, $-30°$)*. The positions are equinox 1950. The B and V magnitudes are in the Johnson system while the R magnitudes are in the Cousins system. The finding chart for this field are in figure 6.*

	R.A.	dec.	B	V	R	Notes
1	13 27 51.2	-32 0 2	16.40	15.75	15.38	*
2	13 27 49.7	-31 58 53	13.97	13.29	12.89	*
3	13 27 49.3	-31 59 31	14.59	13.59	13.08	* †
4	13 27 48.7	-31 59 59	15.05	14.44	14.11	*
5	13 27 48.4	-31 59 11	19.11	18.65	18.34	*
6	13 27 46.3	-32 0 10	16.25	15.45	15.00	* ‡
7	13 27 44.8	-31 59 19	14.26	13.43	12.96	*
8	13 27 44.8	-32 0 21	15.41	14.44	13.87	*
9	13 27 43.8	-31 59 41	17.33	16.55		
10	13 27 43.4	-31 59 47	16.23	15.66		
11	13 27 42.2	-32 0 3	19.45	18.67		
12	13 27 39.5	-31 59 24	20.44	18.93		
13	13 27 39.4	-32 0 25	18.10	17.15		
14	13 27 38.4	-32 0 27	11.71	11.05		

Notes

* Image was measured twice in B and V.

† Double star, separation 7″

‡ Double star, separation 3″.5

TABLE VIII. — *This table gives the normalized response function for the J passband used in this project (IIIa-J, GG395 and UK Schmidt corrector).*

Wavelength/nm	S_λ	Wavelength/nm	S_λ
350	0.00	460	0.80
360	0.01	470	0.79
370	0.11	480	0.78
380	0.36	490	0.77
390	0.63	500	0.83
400	0.76	510	1.00
410	0.81	520	0.92
420	0.83	530	0.70
430	0.78	540	0.31
440	0.73	550	0.14
450	0.76	560	0.05
		570	0.00

TABLE IX. — *This table gives the polynomial coefficients for the relationships between various colours calculated using the stellar spectra in Gunn and Stryker* (1983). *Separate relationships are given for dwarfs and giants. The polynomials are valid in the ranges* $-0.2 < (B-V) < 1.8$, $-0.4 < (B-R) < 3.5$, $-0.4 < (O-E) < 3.3$ *and* $-0.2 < (E-I) < 2.5$. *They have been calculated using an airmass of* 0. C_2 *can then be calculated from the equation* $C_2 = \sum_n a_n\, C_1^n$. *Care should be taken when using these relations for the very reddest stars,* $(B-V) \gtrsim 1.4$.

C_1 → C_2	Stellar Type	a_0	a_1	a_2	a_3	a_4	a_5
(B–V) → (B–R)	Dwarf	-0.004	1.539	0.279	-0.4183	0.1931	—
(B–V) → (B–R)	Giant	-0.007	1.569	0.194	-0.4263	0.1993	—
(B–R) → (R–I)	Dwarf	-0.011	0.452	0.064	-0.3228	0.1824	-0.02644
(B–R) → (R–I)	Giant	-0.017	0.398	0.006	-0.1001	0.0370	—
(O–E) → (B–V)	Dwarf	-0.005	0.526	0.192	-0.1862	0.0645	-0.00761
(O–E) → (B–V)	Giant	0.012	0.526	0.047	-0.0125	—	—
(B–V) → (B–J)	Dwarf	-0.002	0.145	0.230	-0.2787	0.1054	—
(B–V) → (B–J)	Giant	0.005	0.158	0.054	—	—	—
(E–I) → (R–I)	Dwarf	0.005	1.008	-0.007	-0.0293	—	—
(E–I) → (R–I)	Giant	0.008	1.038	-0.098	—	—	—
(O–E) → (O–V)	Dwarf	-0.013	0.686	-0.015	—	—	—
(E–I) → (E–V)	Dwarf	0.008	-0.891	-1.960	3.2500	-1.6779	0.28712
(B–V) → (O–E)	Dwarf	0.006	1.965	-1.363	2.2910	-1.4175	0.30166
(B–V) → (O–V)	Dwarf	0.013	1.415	-1.841	3.2357	-2.1099	0.46438

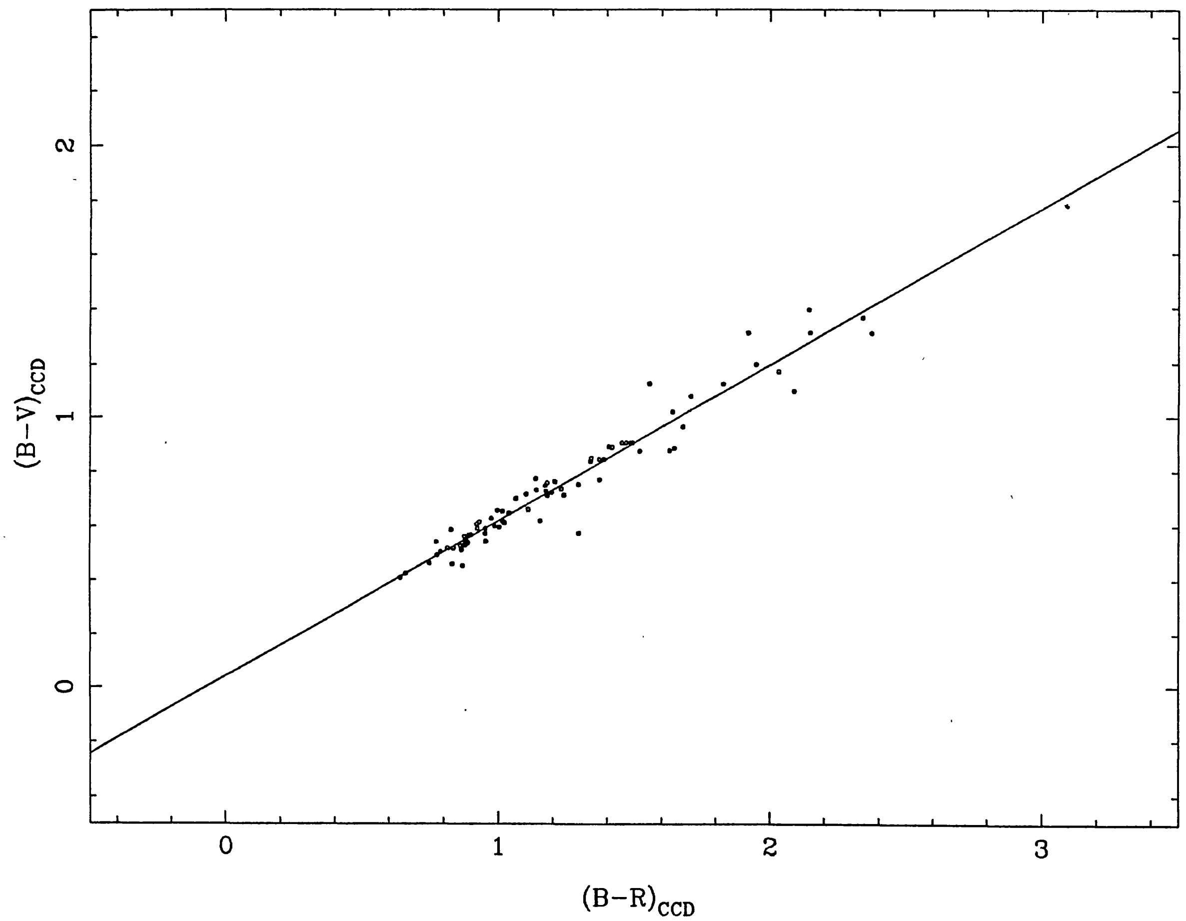

FIGURE 1. — The relationship between $(B-V)_{\mathrm{CCD}}$ and $(B-R)_{\mathrm{CCD}}$ for the filters used on the 1 metre SAAO telescope. The line drawn is a linear fit to the data points.

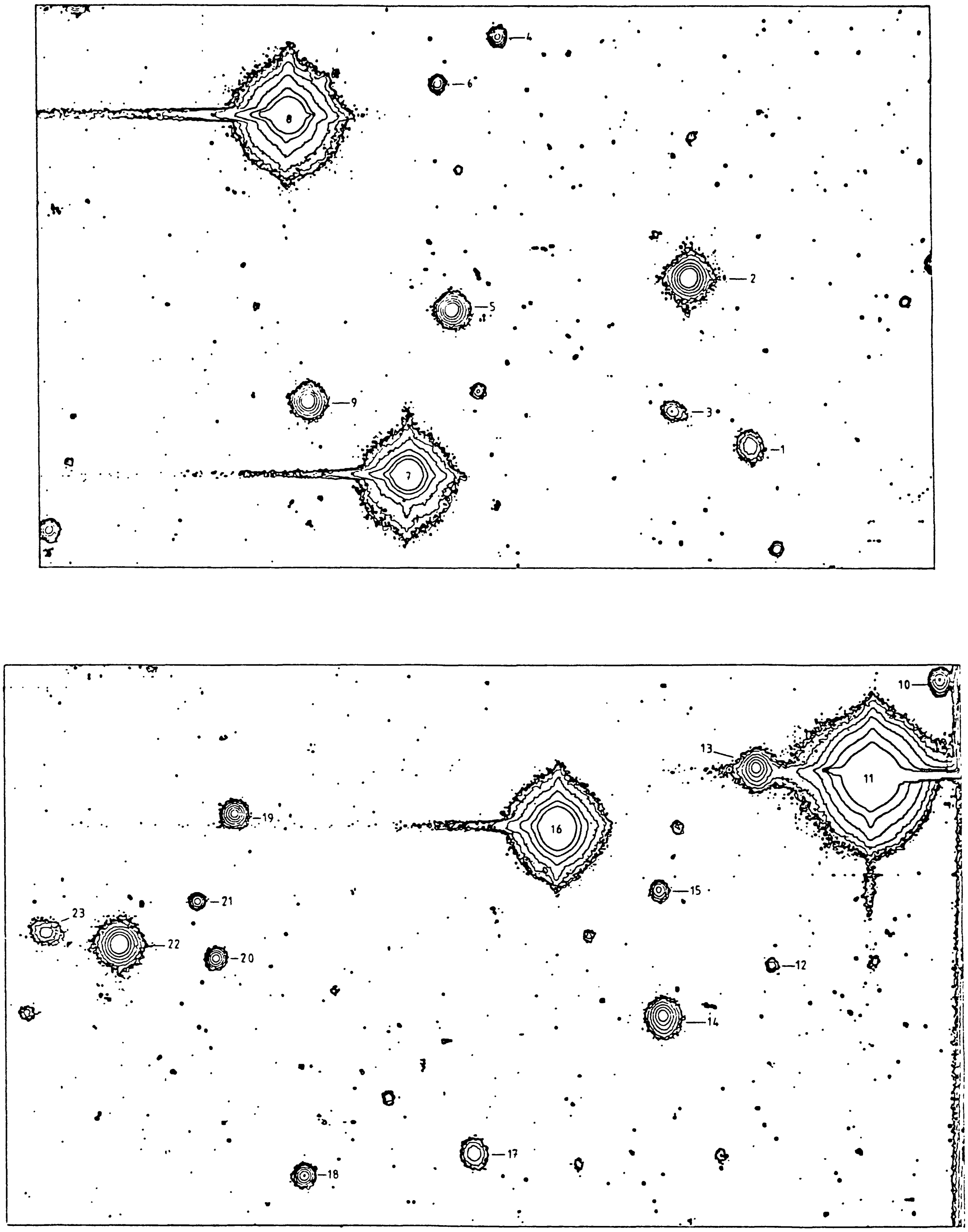

FIGURE 2. — The finding charts for the 8 Hour Field. The orientation is North to the top and East to the right. The size of each finding chart is approximately $2' \times 3'$.

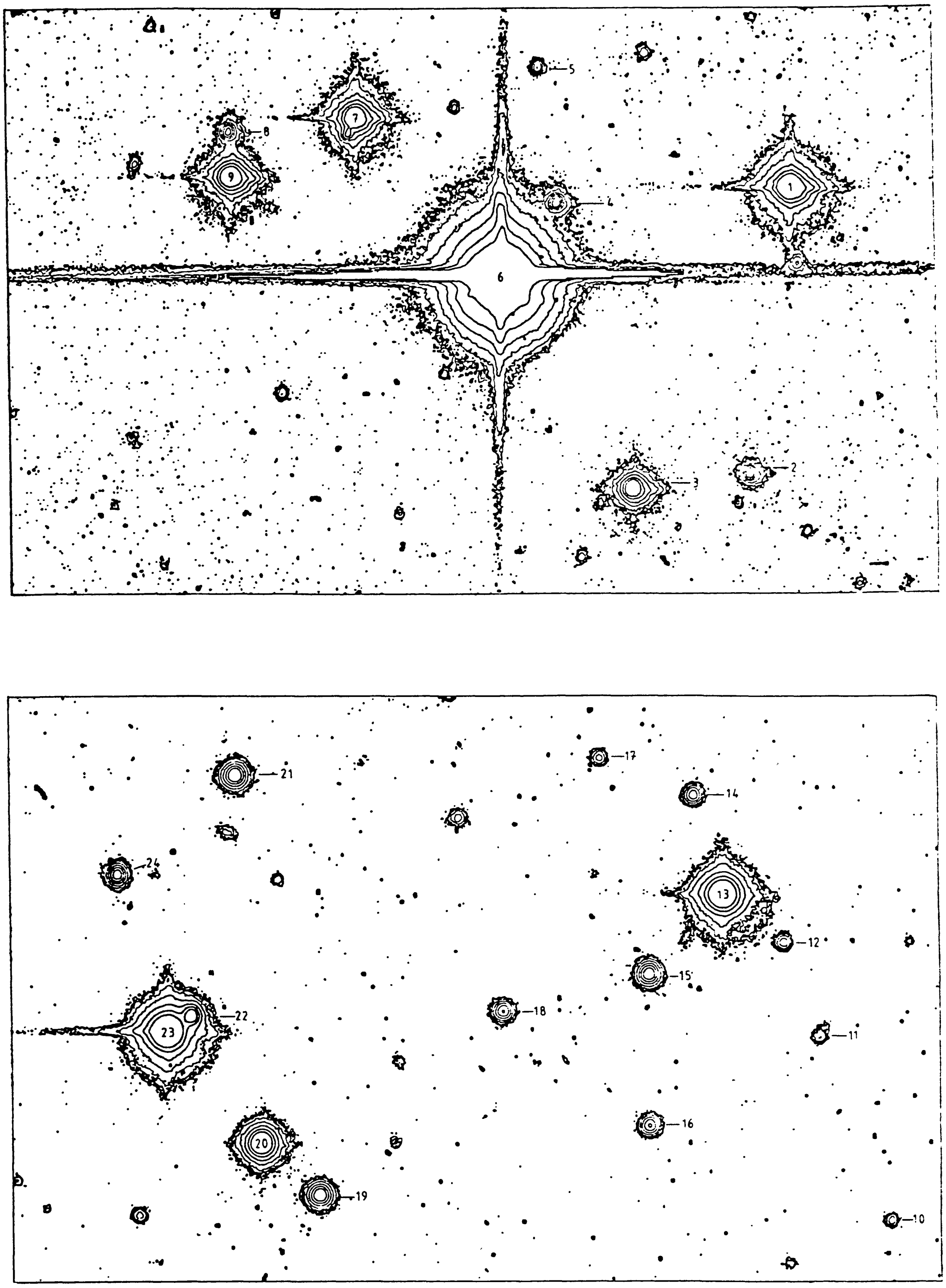

FIGURE 3. — The finding charts for the 11 Hour Field. The orientation is North to the top and East to the right. The size of each finding chart is approximately $2' \times 3'$.

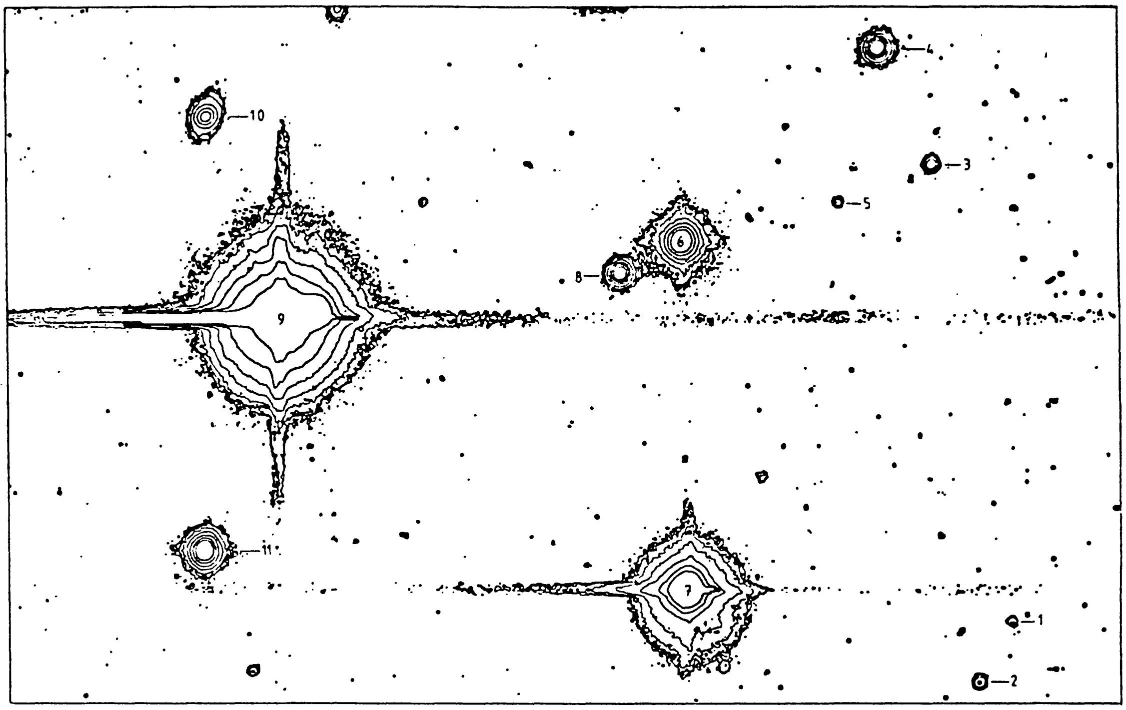

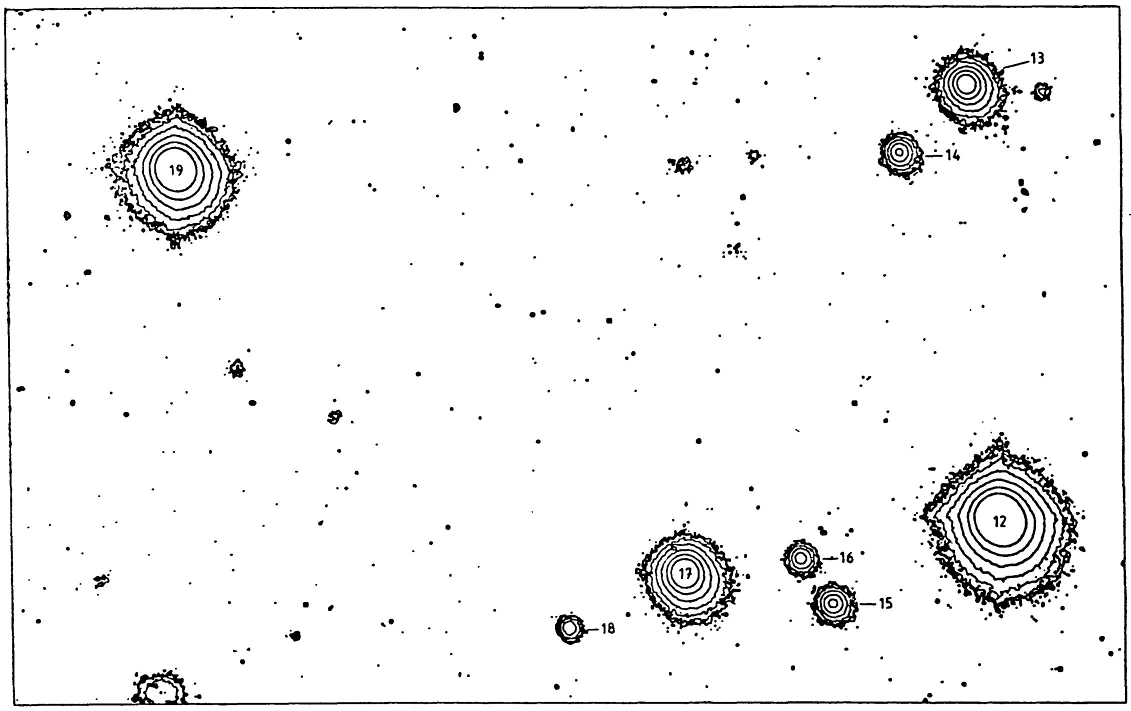

FIGURE 4. — The finding charts for the 12 Hour Field. The orientation is North to the top and East to the right. The size of each finding chart is approximately 2′ × 3′.

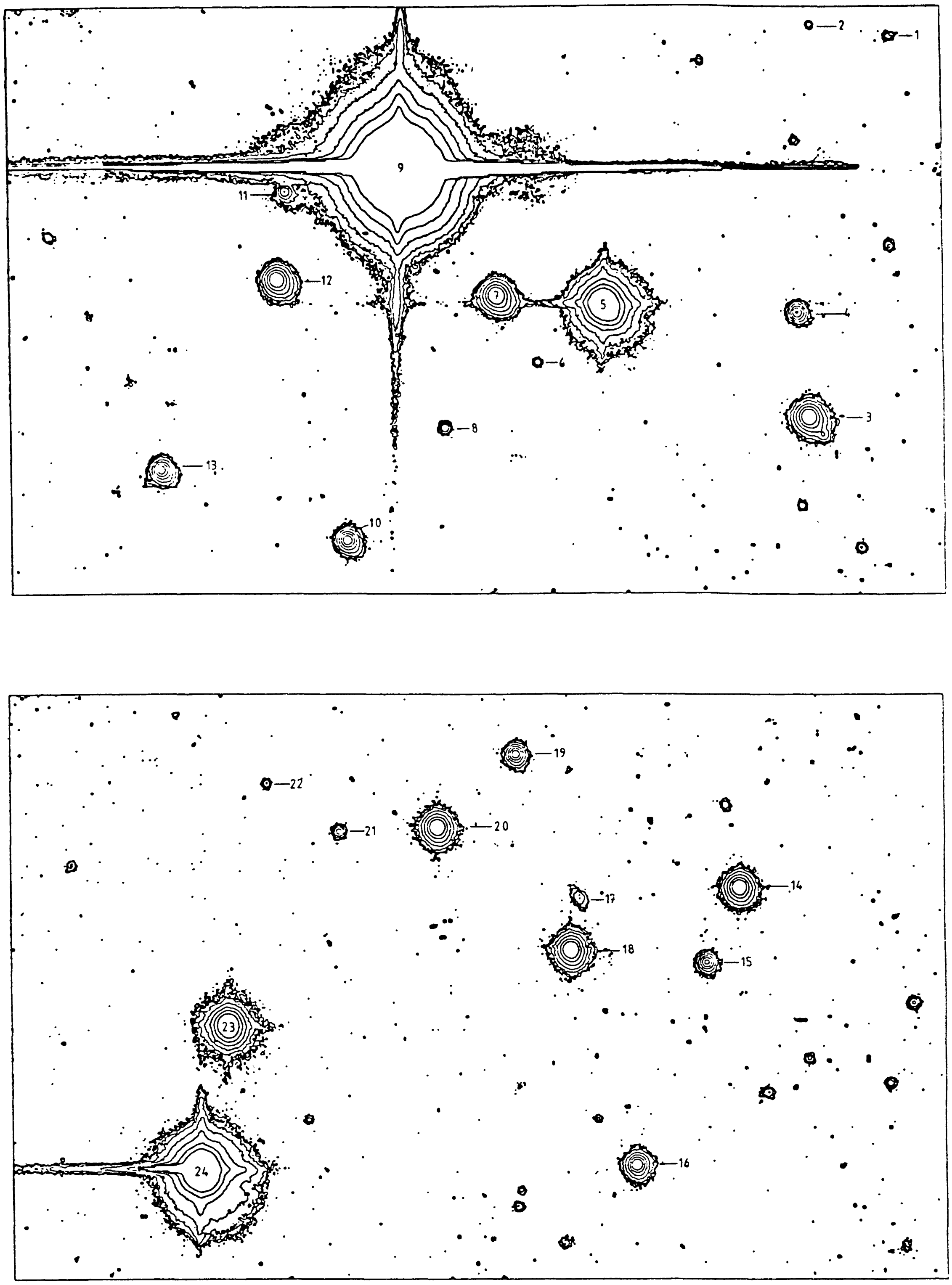

FIGURE 5. — The finding charts for the 15 Hour Field. The orientation is North to the top and East to the right. The size of each finding chart is approximately 2′ × 3′.

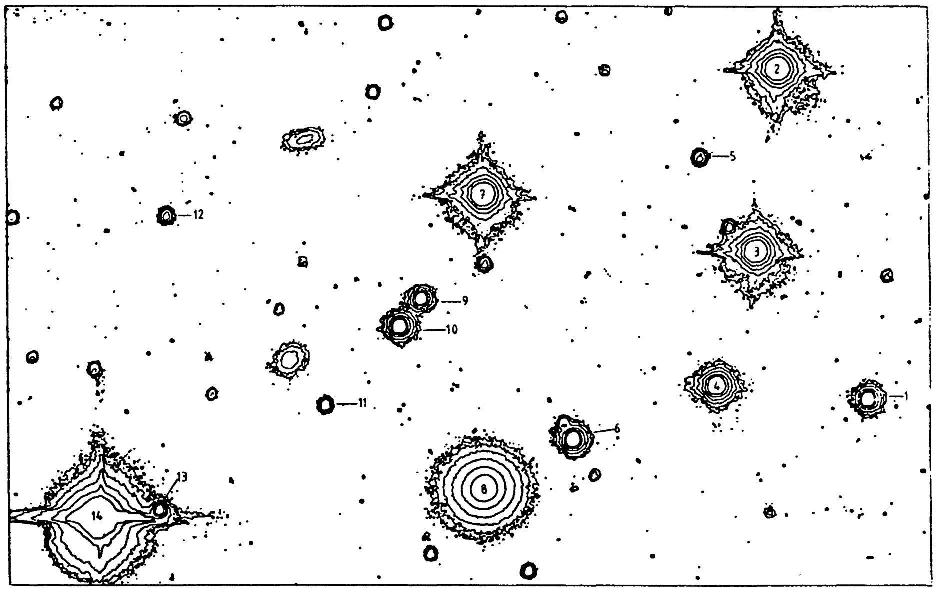

FIGURE 6. — The finding chart for the Additional Field (13^h25^m, $-30°$). The orientation is North to the top and East to the right. The size of each finding chart is approximately $2' \times 3'$.

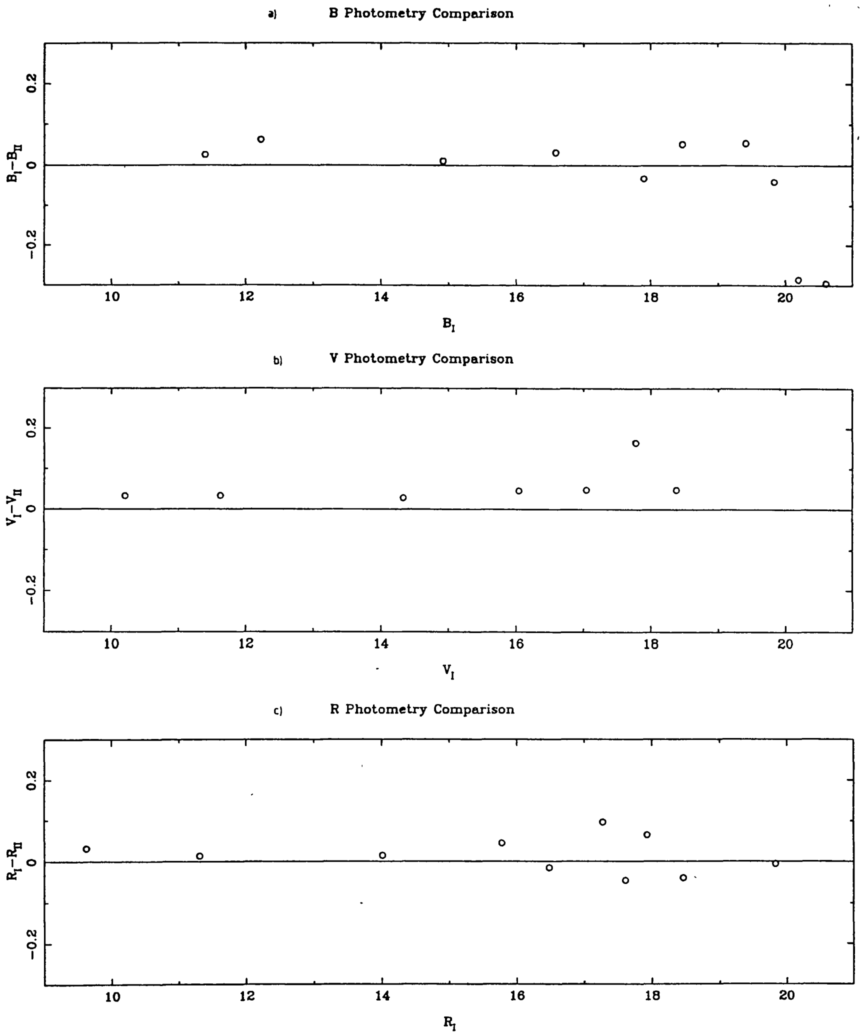

FIGURE 7. — This diagram shows the photometric comparison made for stars in the second CCD region of the 8 Hour Field (star number ≥ 10) for a) B, b) V and c) R. The difference in the magnitudes measured on the two nights is plotted against the magnitude measured on the first night.

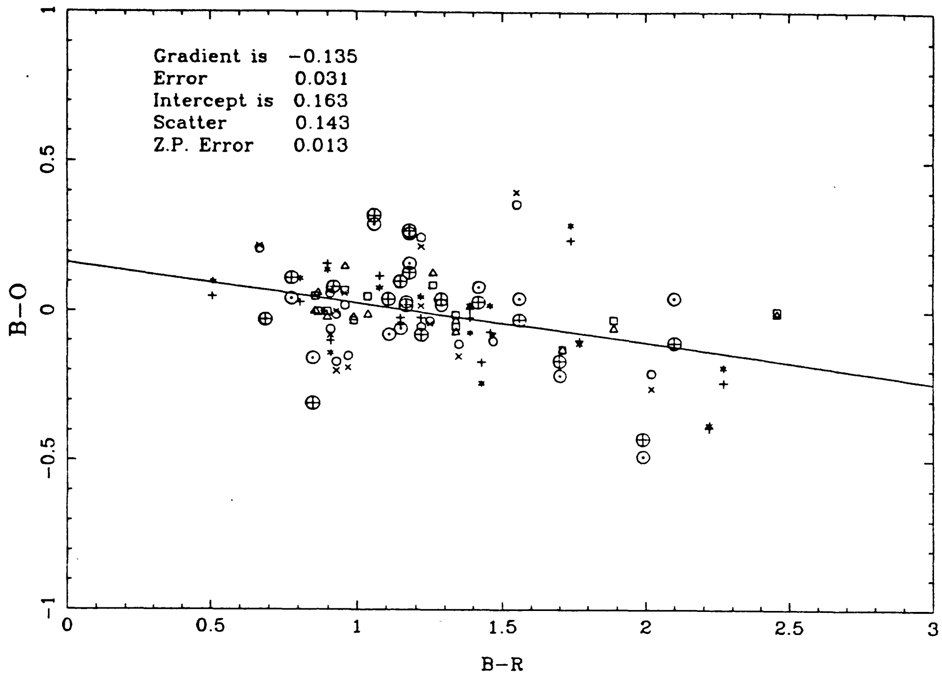

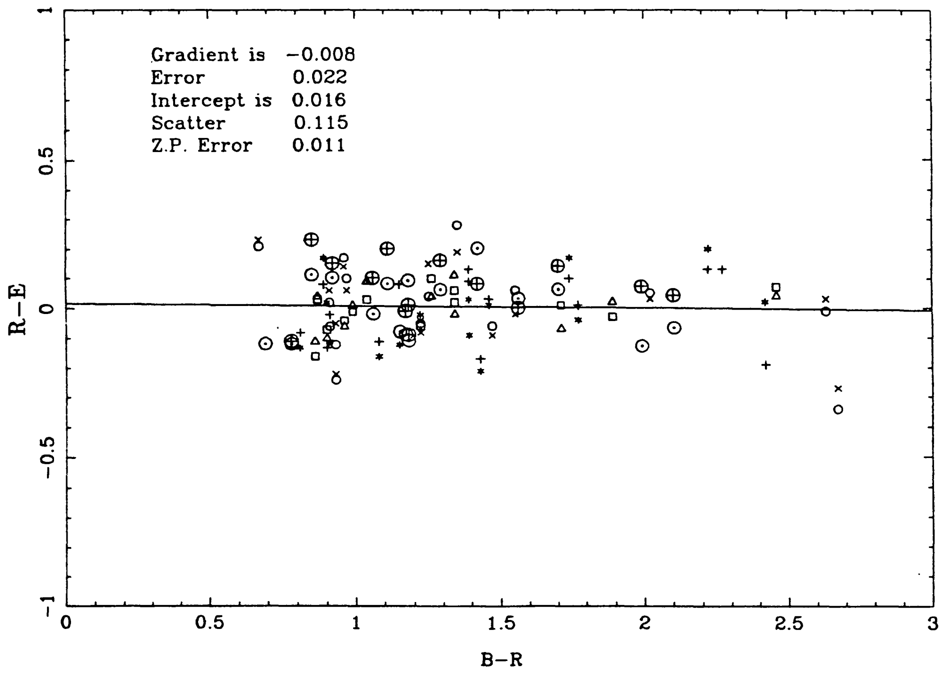

FIGURE 8. — These diagrams show the residuals (i.e. the difference between standard magnitudes and those calibrated from the photographic data) as a function of colour for all CCD standards that are in the 4 project fields. The gradients in these diagrams give the colour terms necessary to convert from the photoelectric (*B*, *R*) system to the photographic (*O*, *E*) one. The different symbols represent data from different fields and scans.

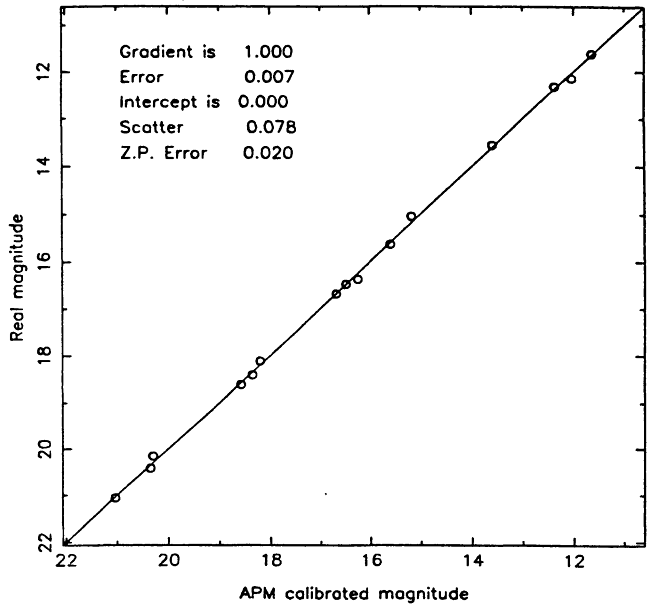

FIGURE 9. — This diagram shows a comparison between CCD magnitudes and magnitudes calculated from the APM data for the standards on the plate O62 (8 Hour Field).

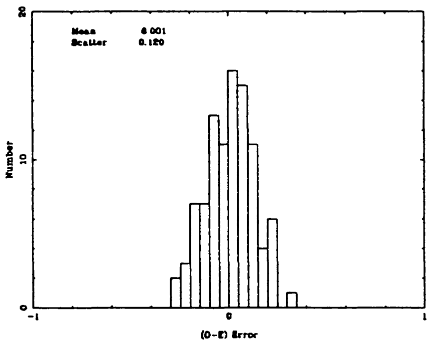

FIGURE 10. — This is a histogram of the colour ($O - E$) errors i.e. CCD colours – colours calculated from the APM data, for the CCD standard stars in all 4 fields for this project.

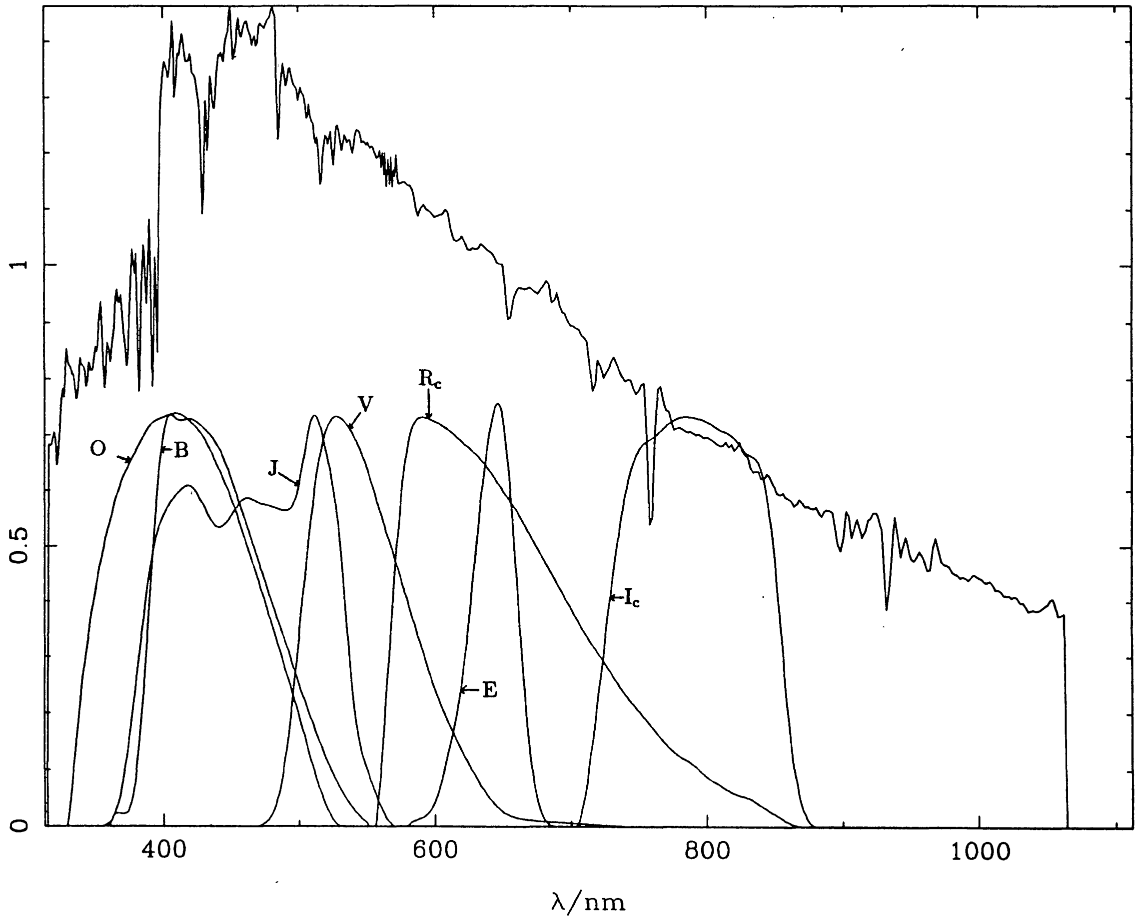

FIGURE 11. — This diagram shows the response functions used in this project superimposed on the spectrum of a G0V star. The ordinate is S_λ or D_λ as appropriate.

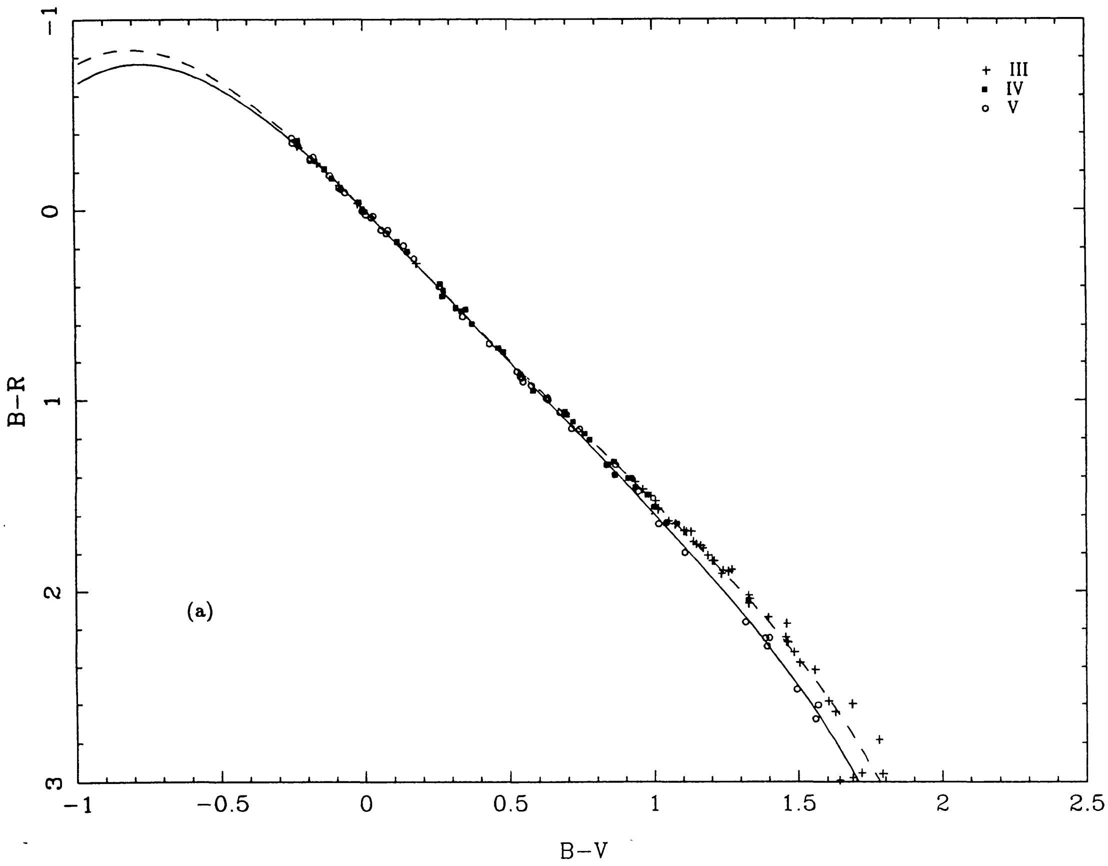

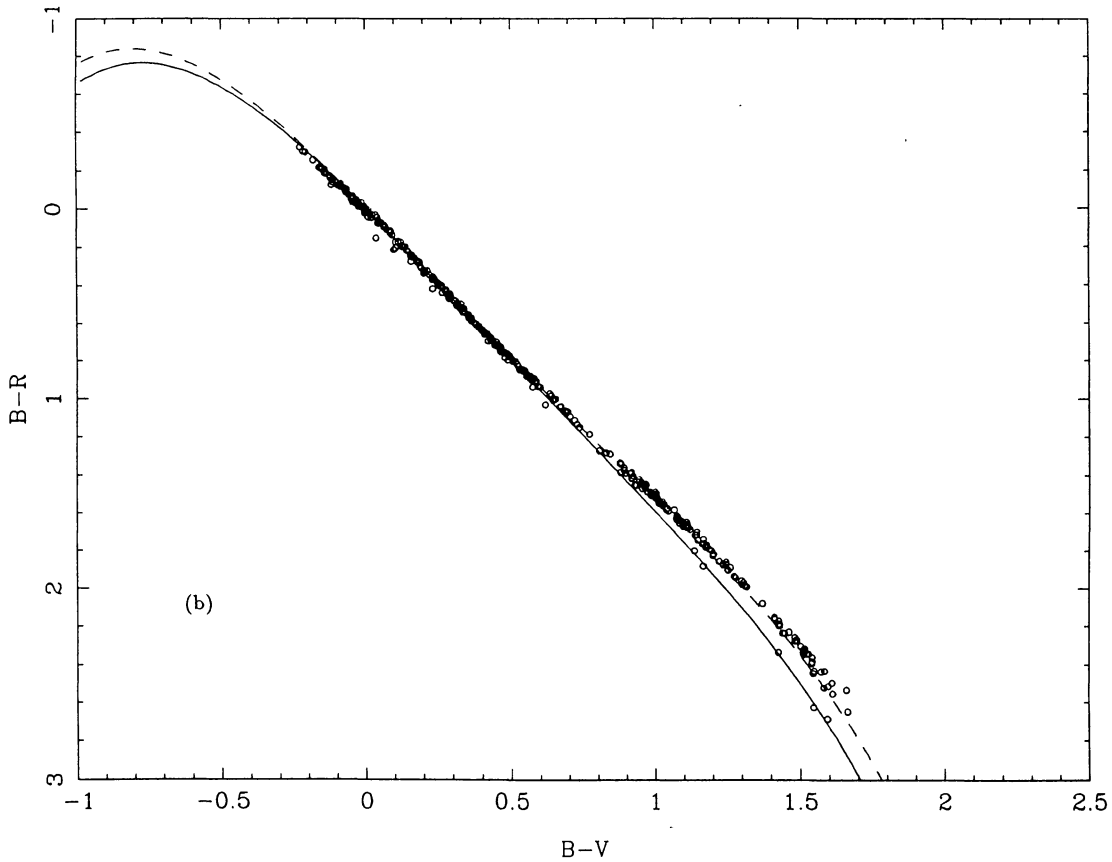

FIGURE 12. — A comparison between synthetic and observed colour-colour relationships. (a) shows the computed relationships between $(B-V)$ and $(B-R)$. The lines drawn are best-fit polynomials for dwarfs (full) and giants (dashed). (b) is the corresponding diagram to (a) and shows the observed relationship. The lines are the same as in (a). (c) and (d) are the same as (a) and (b) but for $(R-I)$ vs. $(B-R)$.

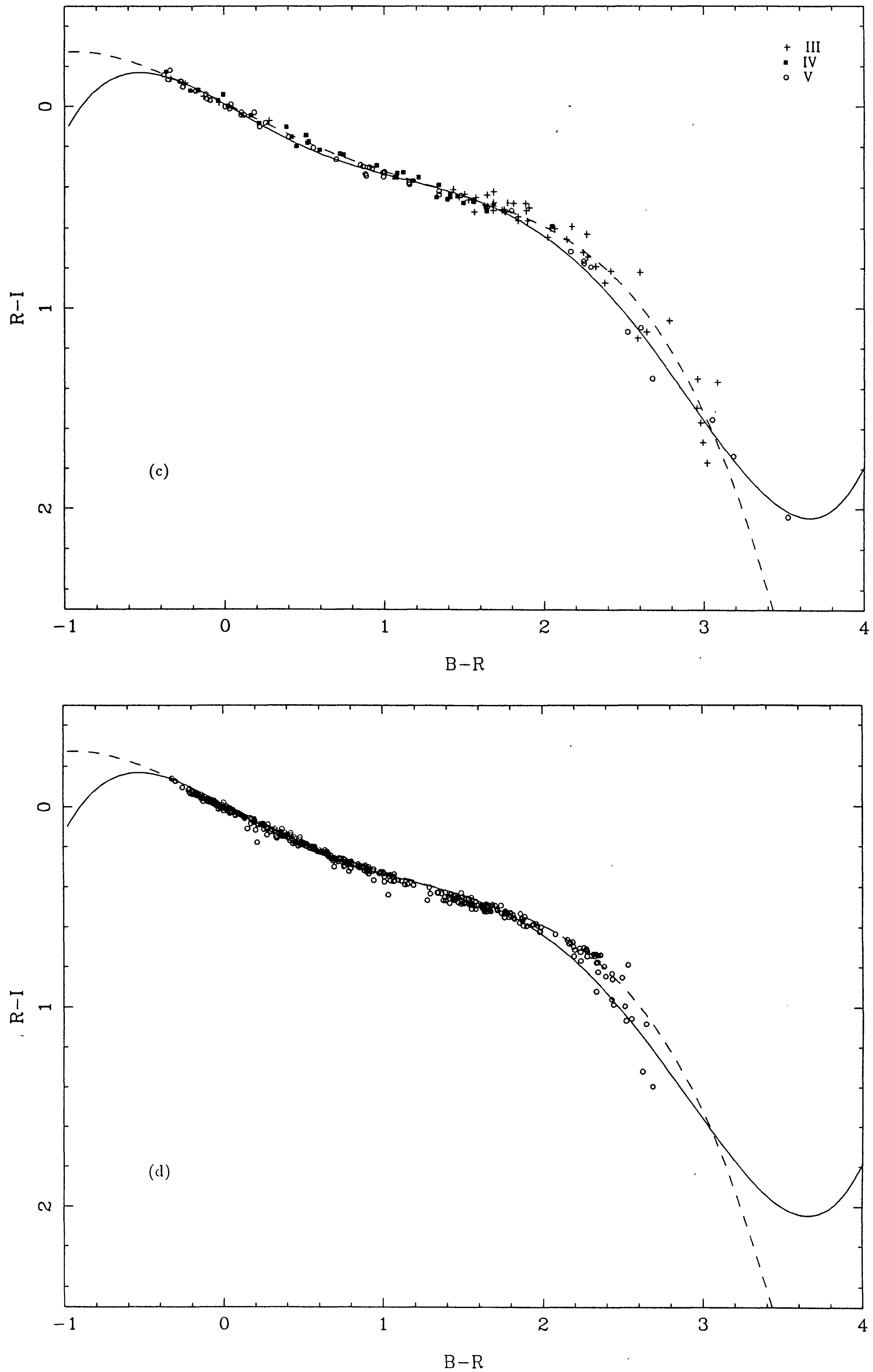

FIGURE 12 (*continued*).

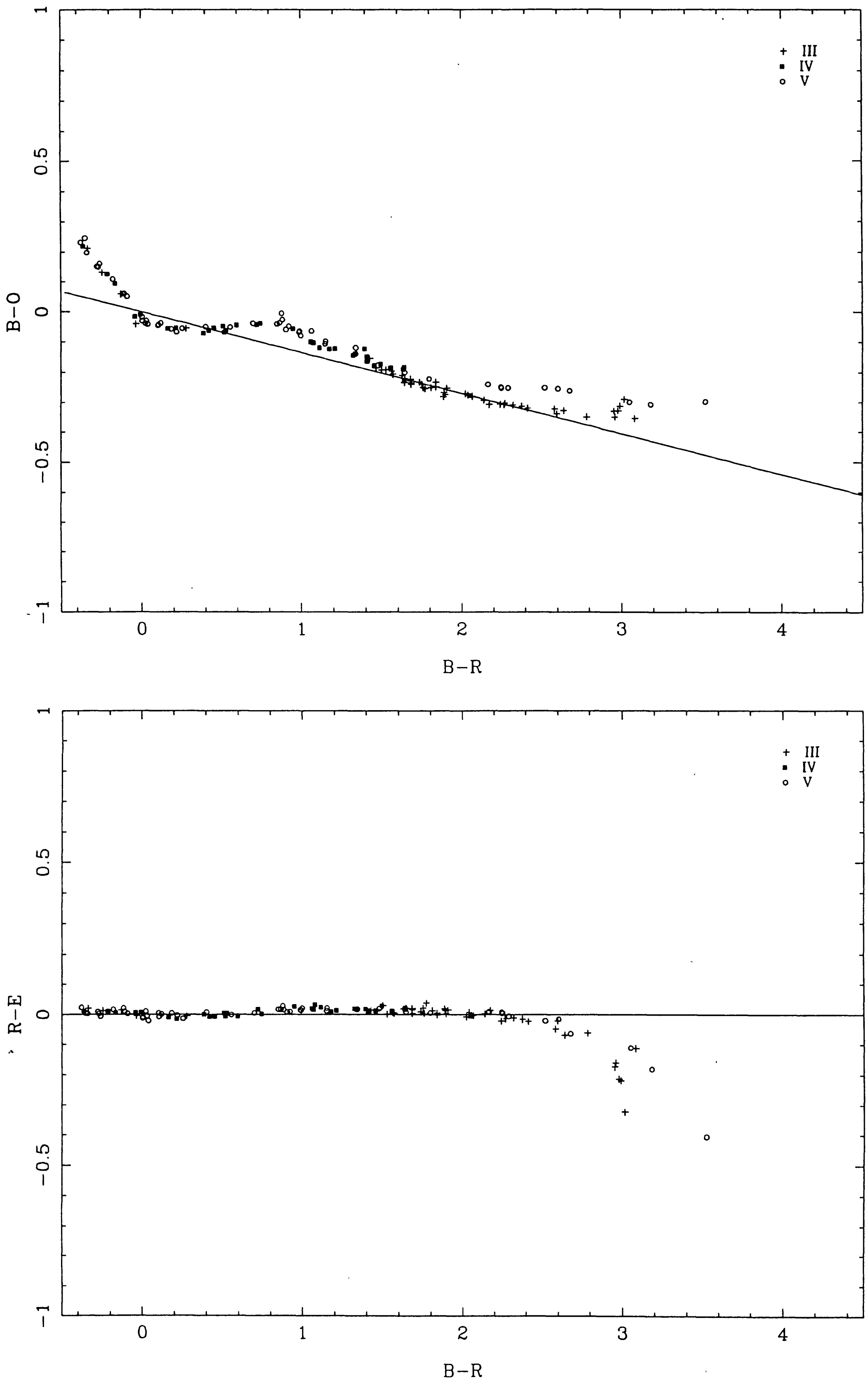

FIGURE 13. — These diagrams illustrate the synthetic relationships for $(B-O)$ (top) and $(R-E)$ (bottom) *vs.* $(B-R)$. The lines drawn are the relationships devired from the CCD standards (Eqs. 11, 12).

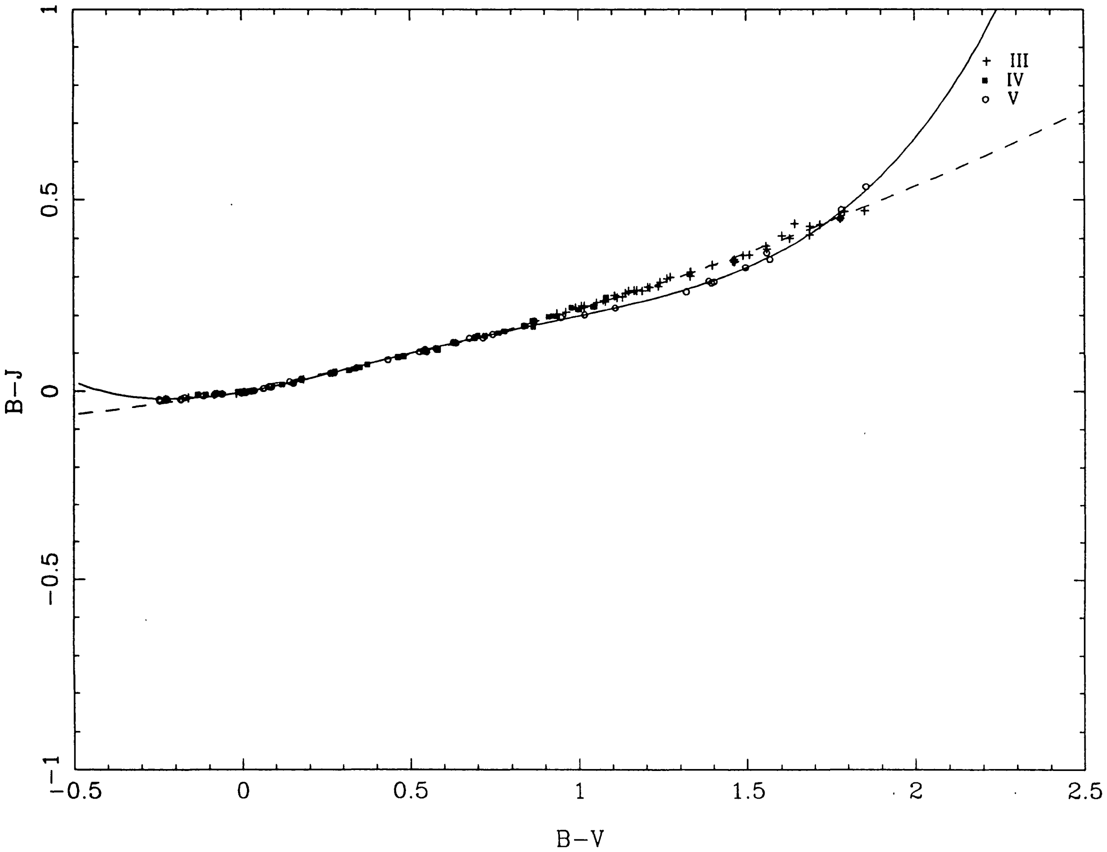

FIGURE 14. — This diagram shows the relationship between $(B-J)$ and $(B-V)$ derived from stellar spectra. The solid line is the dwarf relationship and the dashed line is for giants. The coefficients for these polynomials are given in table IX.

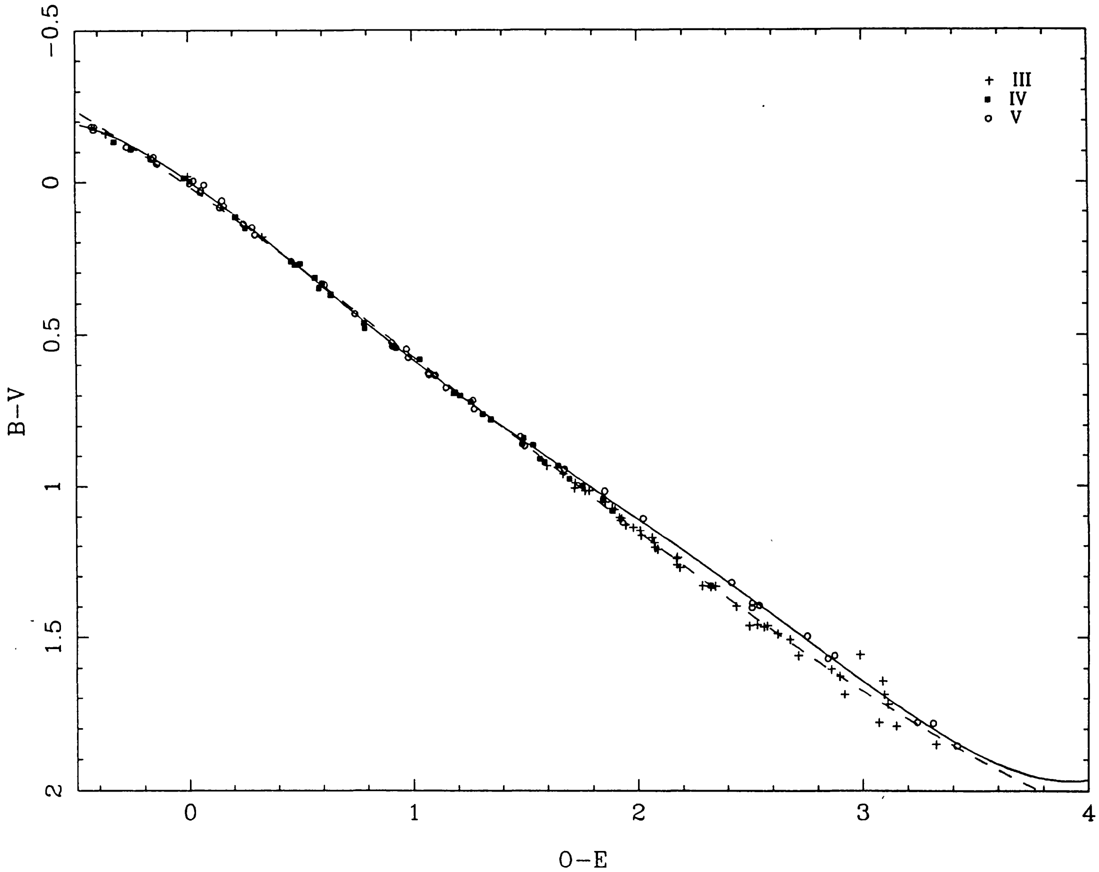

FIGURE 15. — Same as figure 14 except for $(B-V)$ vs. $(O-E)$.

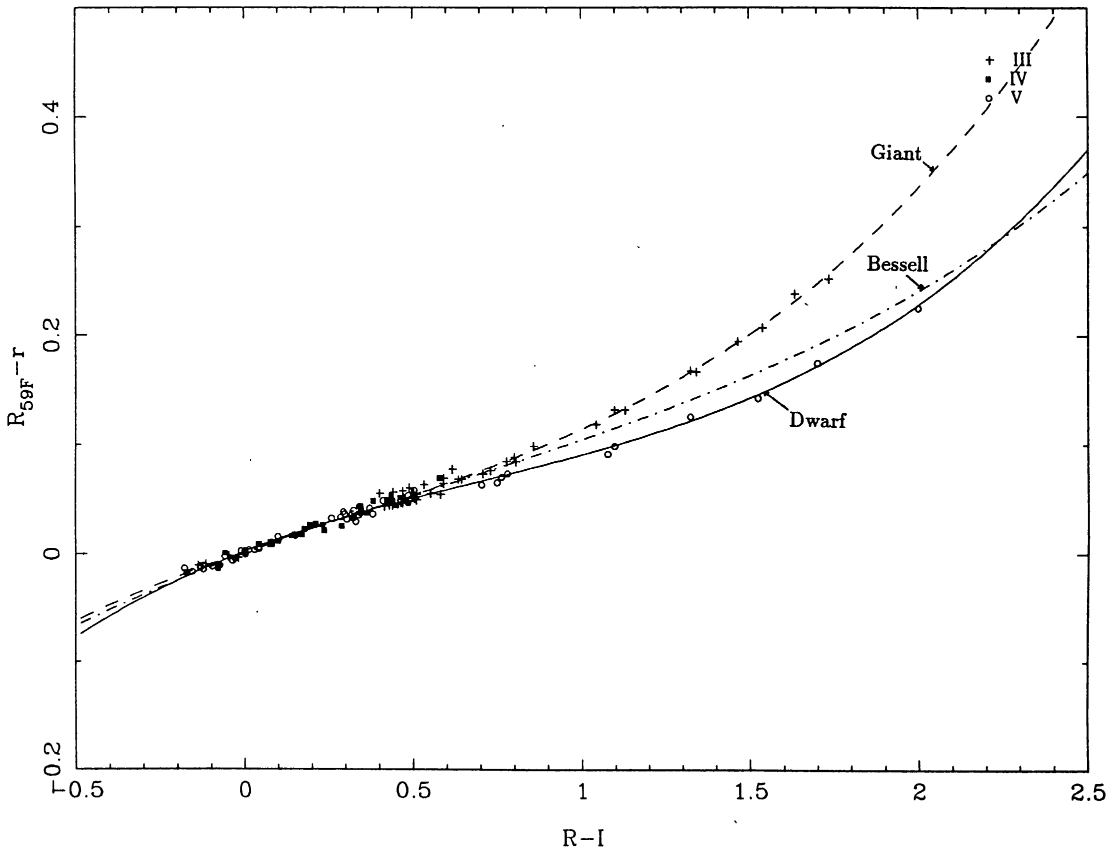

FIGURE 16. — This diagram shows a comparison between this work and that of Bessell (1986). The passbands R_{59F} and r are given in this paper. The best-fit polynomials for dwarfs and giants are drawn along with the relationship derived by Bessell.